Table 1 Parameters for voltage dependence of steady-state activation and steady-state inactivation of the DRG-type sodium channels

	Steady-state activation		Steady-state inactivation		
	$V_{1/2\text{-}a}$	K_a	$V_{1/2\text{-}i}$	K_i	n
Control	−30.0 ± 1.22	6.90 ± 0.54	−71.9 ± 0.90	6.97 ± 0.66	6
BmK I	−42.0 ± 1.31*	7.05 ± 0.52	−75.6 ± 1.07	10.25 ± 0.64	5
BmK I-mix	−48.6 ± 1.40**	3.29 ± 0.49*	−76.8 ± 0.62	9.26 ± 0.33	5
Control	−25.7 ± 1.81	4.27 ± 0.59	−69.2 ± 1.12	7.78 ± 0.67	6
BmK IT2	−38.1 ± 0.98*	4.48 ± 0.38	−72.2 ± 0.86	7.91 ± 0.36	5
BmK IT2-mix	−30.1 ± 1.74	5.81 ± 0.73	−71.6 ± 1.06	9.84 ± 0.56	5

*$p < 0.05$, **$p < 0.01$, significant difference to control (one-way ANOVA, Tukey test)

while it was 4.223 ± 0.4944 ms ($n = 10$), 4.902 ± 0.6564 ms ($n = 10$) and 5.203 ± 0.6961 ms ($n = 10$) in control (Fig. 4a). In addition, the open-state inactivation of VGSCs in BmK I-mix group was still slower than in control group with the time constant of 6.306 ± 0.3762 ms ($n = 6$, $p < 0.05$), 6.371 ± 0.4289 ms ($n = 6$, $p < 0.05$) and 6.499 ± 0.4195 ms ($n = 6$, $p < 0.05$) at 10 mV, 20 mV and 30 mV (Fig. 4a). BmK IT2-mix group was shared an similar property, and the time constant was 6.710 ± 0.7331 ms ($n = 9$, $p < 0.05$), 7.284 ± 0.5559 ms ($n = 9$, $p < 0.05$) and 7.320 ± 0.6516 ms ($n = 9$, $p < 0.05$) in BmK IT2-mix group compared to 4.666 ± 0.5358 ms ($n = 9$), 5.899 ± 0.6654 ms ($n = 9$) and 5.499 ± 0.6426 ms ($n = 9$) in control group (Fig. 4b). BmK IT2 did not prolong the time constant of open-state inactivation, whose time constant was 4.854 ± 0.7474 ms ($n = 5$, $p > 0.05$), 5.138 ± 0.5182 ms ($n = 5$, $p > 0.05$) and 6.479 ± 0.8902 ms ($n = 5$, $p > 0.05$) (Fig. 4b).

Discussion

In this study, the positive synergistic effect of BmK I and BmK IT2 on ND7-23 endogenous VGSCs was identified by whole cell patch clamp. From our results, we found out that BmK IT2 enhanced the pharmacological effect of BmK I by eliciting a higher peak current (Fig. 1c) and shifting the voltage-dependent activation to more hyperpolarized potential (Fig. 2a). The steady-state inactivation of VGSCs was not affected by co-applying BmK I and BmK IT2 (Fig. 3), which indicated that positive synergistic effect brought no extra effect on other pharmacological properties of sodium channels. It has been reported that the performance of site-3 toxins was enhanced by site-4 toxins in insects based on toxicity assays and binding experiments [15]. Our work provides another evidence of positive synergistic effect induced by two toxins on mammalian VGSCs by studying the modulation of gating properties, not the toxicity or binding experiments as previously done [15].

BmK I acts as a receptor site-3 modulator while BmK IT2 modulates sodium channels by binding to receptor site 4. It has been reported that the sensitivity of the receptor site 3 can be enhanced by specific ligands of another receptor site. For instance, brevetoxin (Pbtx-1) bound to receptor site-5 has positive allosteric modulation on LqhαITa site-3 toxin binding to insect sodium channels [16, 17]. In this case, we speculated that BmK IT2 seems to play a similar role as Pbtx-1. BmK IT2, binding to receptor site 4, may induce a conformational change on the channels. Moreover, the conformational change of channels not only modulates gating properties but also affect the binding of BmK I to receptor site 3. As was previously reported, receptor site 4 is mainly assigned to the S3-S4 in domain II, whereas site 3

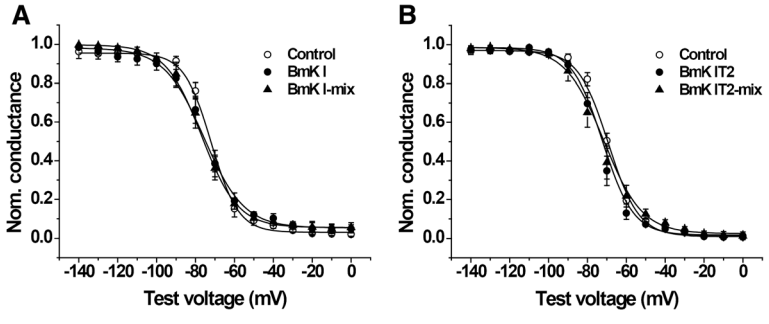

Fig. 3 Effect of BmK I and BmK IT2 on the voltage dependence of steady-state inactivation. **a** The G-V curve of the steady-state inactivation in the absence ($n = 6$), presence of 400 nM BmK I ($n = 5$) and in presence of 400 nM BmK I and 400 BmK IT2 ($n = 5$). **b** The G-V curve of the steady-state inactivation in the absence ($n = 6$), presence of 400 nM BmK IT2 ($n = 5$) and in presence of 400 nM BmK I and 400 BmK IT2 ($n = 5$)